

Supplementary Information.

Protein monolayer formation: the combined role of the surface features and protein-protein interactions

Paola Campione,^{av} Grazia ML Messina,^{av} Micaela Giannetti,^b Claudia Mazzuca,^{b*} and Antonio Palleschi.^{b*}

^a *Laboratory for Molecular Surfaces and Nanotechnology (LAMSUN), Department of Chemical Sciences, University of Catania and CSGI, Viale A.Doria 6, 95125 Catania, Italy.*

^b *Department of Chemical Science and Technologies, University of Rome "Tor Vergata", Via della Ricerca Scientifica, 00133 Rome, Italy.*

^v: they have contributed equally.

*: corresponding authors: E mails: AP: antonio.palleschi@uniroma2.it; CM: claudia.mazzuca@uniroma2.it.

Materials and Methods

Validation of the PMMA surface model

To validate the use of a PMMA surface modelled with a mixed Martini CG/atomistic OPLS force field (hereafter referred to as the 'mixed' model), two different tests were performed.

In the first one, short-range interactions between the PMMA surface and the single protein were compared. To this end, two different 100 ns long MD simulations were performed using, in one case, the mixed model and in the other one explicitly considering all atoms. In both cases, at the beginning of the simulation, the protein was placed in water, close to the surface (a minimum distance of 1.2 nm), with the same orientation. At the end of the simulation, as shown in Figure S1A, the LYZ conformations are very similar and, in both cases, the proteins are well anchored on the PMMA surface (Figure S1B). Furthermore, both the dynamic fluctuations of the protein, as shown by the root mean square fluctuations (RMSF) of the C α atoms (Figure S2A) and the solvent accessible surface area (SASA) as reported in Figure S2B, are very similar. The data obtained (Figures S1–S2) strongly support the fact that the mixed model, less expensive in terms of computational time, can provide very similar results to the one in which all atoms are explicitly considered.

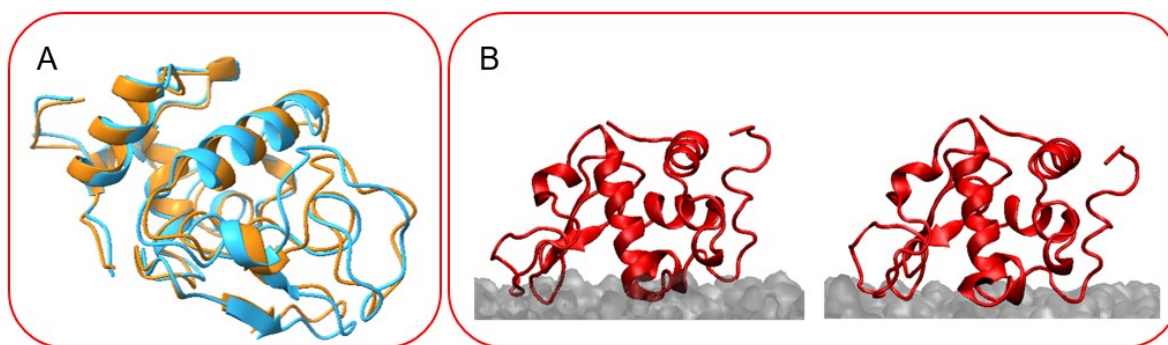


Fig. S1 (A): snapshots of LYZ protein after 100 ns MD simulation in the presence of PMMA modelled according to a 'mixed' (light blue) or an all-atom force field approach (orange); (B): side view snapshots at the end of simulations of a LYZ molecule on PMMA modelled with (sx) a 'mixed' or (dx) an all-atom force field. Proteins are in red, while PMMA in grey.

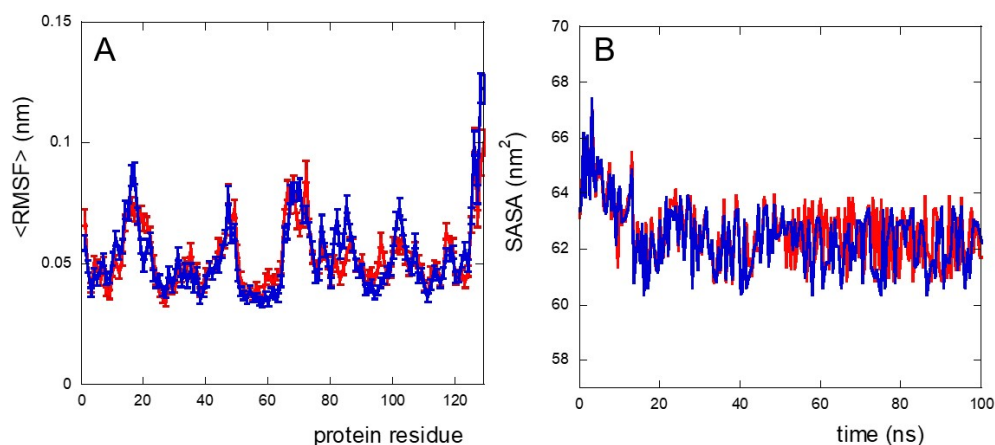


Fig. S2 (A): Average values of RMSF (root mean square fluctuations) for each C α atom in the LYZ protein found in the last 10 ns of MD simulations and (B): values of SASA (Surface Accessible Solvent Area) for LYZ during all 100 ns MD simulations, in the presence of a PMMA surface modelled with a 'mixed' (red) or an all-atom force field (blue).

A second series of MD simulations was performed, which aimed at also considering protein-protein interactions (see the main text for details), which are of great importance in the process of protein adsorption on the surface. In detail, a first MD simulation of 15 LYZ molecules on a PMMA surface described using the 'mixed' model was performed. Then, keeping the same final configuration of the proteins, the mixed force field was replaced with the one with all-atom explicit for the surface, and a further MD simulation (50 ns long) was performed. Interestingly, the SASA per protein, in the case of the all-atom surface, was found to be equal to 60.64 ± 0.34 practically coinciding with that obtained in the case of the mixed model (60.96 ± 0.26 , see Table 6 reported in the main text). Furthermore, as shown in Figure S3, modifying the force field used to describe the PMMA surface does not substantially alter either the surface configuration of the adsorbed proteins (Figure S3A) or their dynamic fluctuations (Figure S3B).

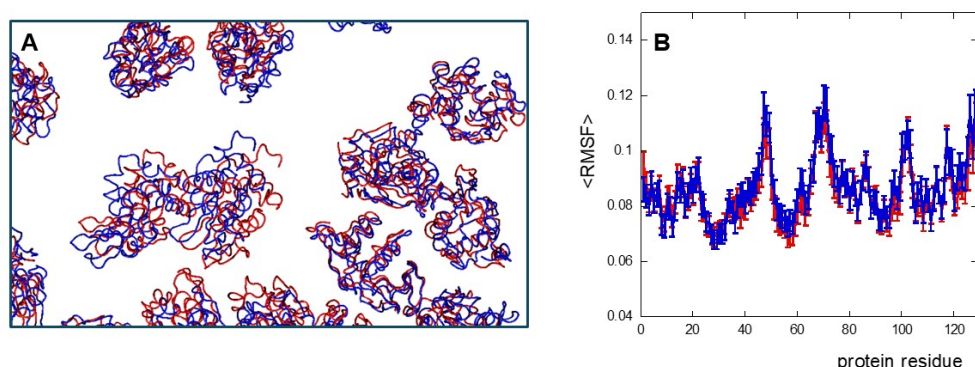


Fig. S3 (A): Top view images of the last snapshot of MD simulations of 15 LYZ molecules adsorbed on PMMA modelled according to a "mixed" (red) or an all-atom force field (blue); (B): average RMSF values for C α atoms of the LYZ proteins in the last 10 ns of MD simulations in the presence of a PMMA surface modelled with a 'mixed' (red) or an all-atom force field (blue).

MD simulations of proteins on surfaces.

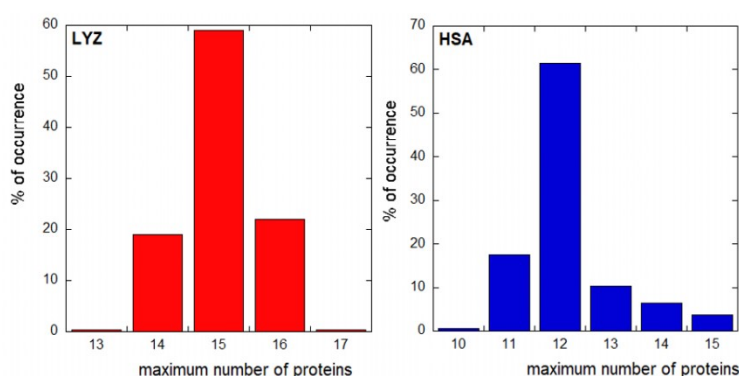


Fig. S4 Distribution of the maximum number of proteins randomly entering on the surface of the simulation box without short contacts for (*sx*): LYZ (surface 17x12nm²); (*dx*): HSA (surface 29x30 nm²).

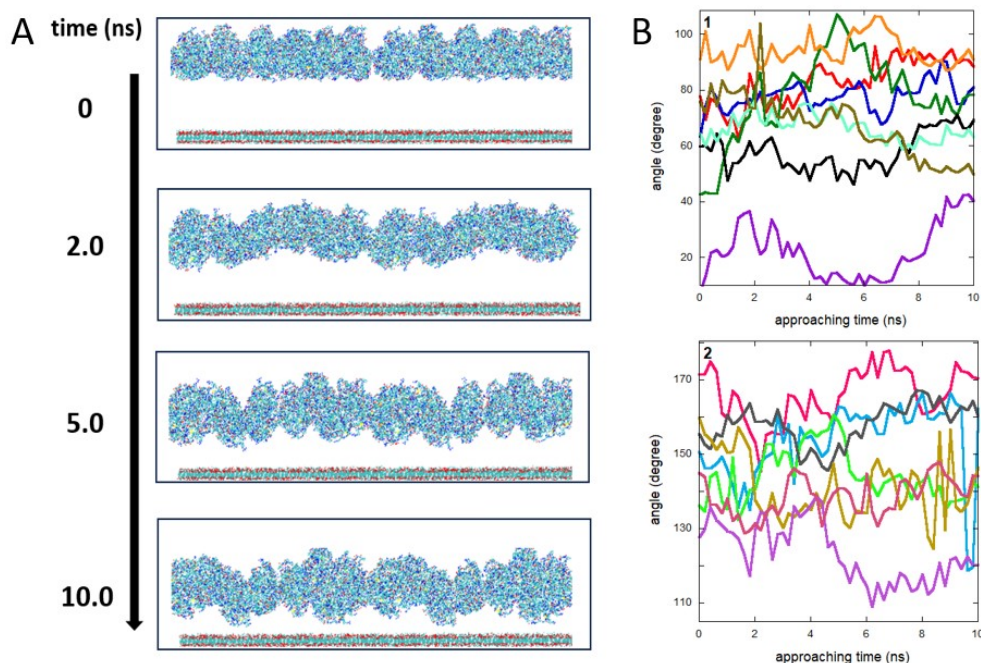


Fig. S5 (A): side view of snapshots of MD simulations, during time, of 15 LYZ molecules approaching the PMMA surface; (B): variation during time, when approaching the surface, of the angle between the longest axis of each LYZ molecules and the Z axis perpendicular to the surface. Data are divided into two panels, 1 and 2, for clarity. Colours refer to different proteins.

$$W_{exp} = \frac{(MW_{prot} + 18 \cdot n_c) \cdot np}{f_{p_tot}} \cdot 0.166054 \frac{ng}{cm^2} \quad (S1)$$

“Validation of the MD protocol on simulating proteins adsorption on surface”

To test the validity of our MD protocol, we compared our result with that obtained using a very different approach. In detail, Fig. S6 reports the angle between the dipole moment of the 15 LYZ molecules, adsorbed on the gold surface, and the positive Z-axis of the simulation box during the MD simulation used in this work. As shown, in the last 30 ns of simulation, this angle is $(87 \pm 10)^\circ$ in good agreement with the result obtained by Zhang et al¹ $(90.36 \pm 4.98)^\circ$, using a different computational method (MM-PBSA), for a simpler system containing a single LYZ molecule on the gold surface.

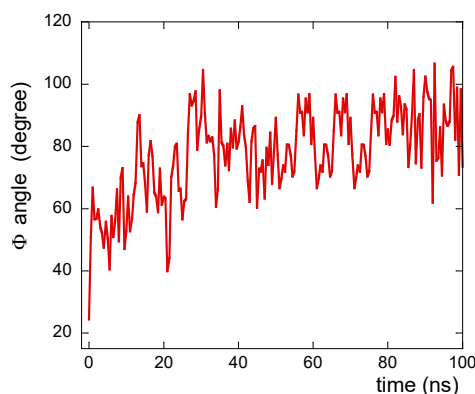


Fig. S6 Value of the angle between the total dipole moment vector of the 15 LYZ molecules and the Z-axis normal to the gold surface.

We also investigated how the number of adsorbed proteins and their orientations influence the results obtained. In other words, we intended to test the statistical robustness of the systems studied.

For the sake of comparison, the more crowded system with 15 molecules of HSA has also been simulated (as shown in Fig. S1, it is possible to obtain a monolayer with up to 15 HSA molecules). In this case, the SASA *per* protein value obtained in the last 10ns of the simulations is 291.2 ± 2.2 , while in the case of 12 HSA the SASA *per* protein is found to be 290.19 ± 0.80 (see also Table 6 in the main manuscript). Furthermore, the number of contacts *per* protein between proteins and the surface (to estimate the protein-surface contact, we considered all the atoms of the protein at a distance less than 0.5 nm from the surface) is about 1737 and 1780 in the case of systems with 15 and 12 HSA, respectively. Finally, also the calculated water charge densities as a function of distance from the gold surface obtained by MD simulation with 12 or 15 HSA are very similar, as shown in Fig. S7, demonstrating that the charge distribution of the water molecules is not significantly influenced by the number of proteins adsorbed.

All these data indicate that the results obtained with 15 HSA are comparable to those obtained in the case of 12 proteins, and therefore do not depend on the starting conditions (number of proteins and different orientations). This in turn strongly suggests that the approach used in this work is statistically significant.

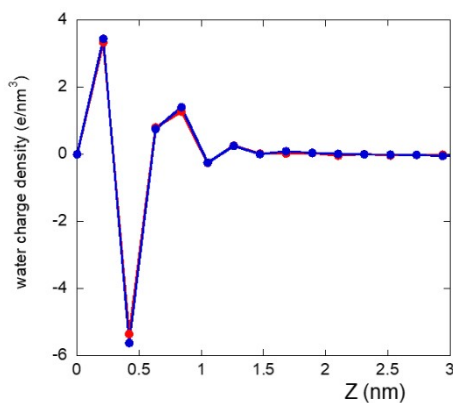


Fig. S7 Water charge density as a function of the distance from the gold surface (Z) for systems containing 12 HSA (red) or 15 HSA (blue) in the simulation box.

Results and Discussion.

Table S1. Slope values (s) obtained by plotting changes in frequency and dissipation (F_3 and D_3 , the more sensitive) against each other, DF plot, of HSA and LYZ on gold and PMMA surfaces.

	HSA/Au	HSA/PMMA	LYZ/Au	LYZ/PMMA
Slope I (s)	$1.73 \cdot 10^{-8}$	$4.30 \cdot 10^{-8}$	$1.2 \cdot 10^{-8}$	$2.40 \cdot 10^{-8}$
Slope II (s)	$5.55 \cdot 10^{-8}$	$5.46 \cdot 10^{-8}$	-----	-----
Slope III(s)	$2.98 \cdot 10^{-8}$	-----	-----	-----

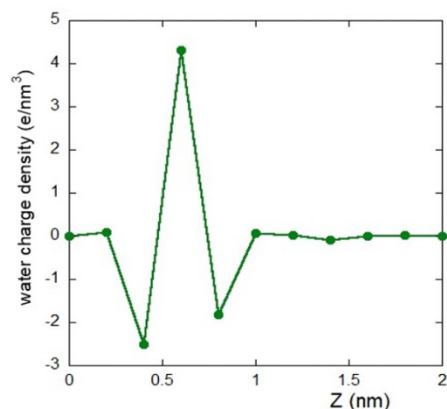


Fig. S8 Water charge density as a function of the distance from the gold surface (Z) for the system in absence of adsorbed proteins.

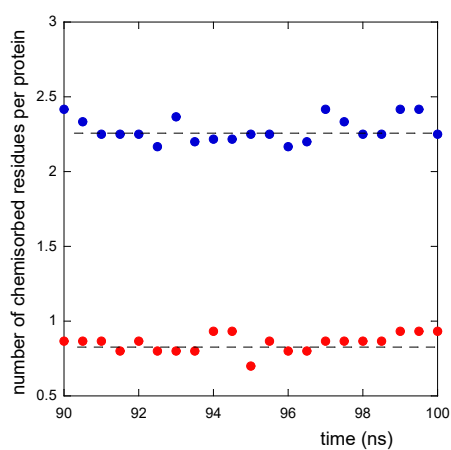


Fig. S9 Number of chemisorbed residues *per* protein for HSA (blue) and LYZ (red) in the last 10 ns of simulation. The dotted line are a guide for eyes.

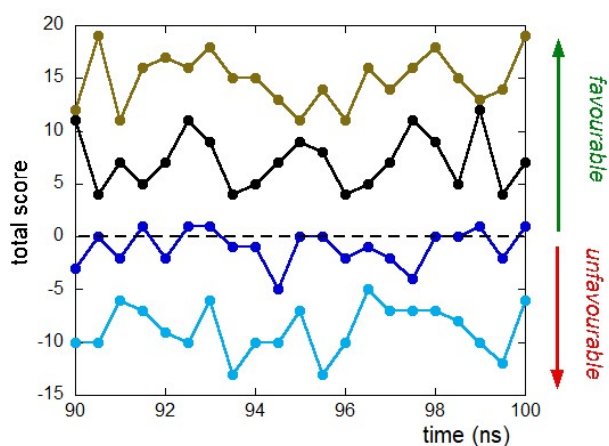


Fig. S10 Total score of hydrophobic (for HSA: light blue; for LYZ: brown) or charge-charge (for HSA: blue; for LYZ: black) interactions during the last 10 ns simulation time on PMMA. See the main text for details. The dotted line at zero is only a guide for the eyes.

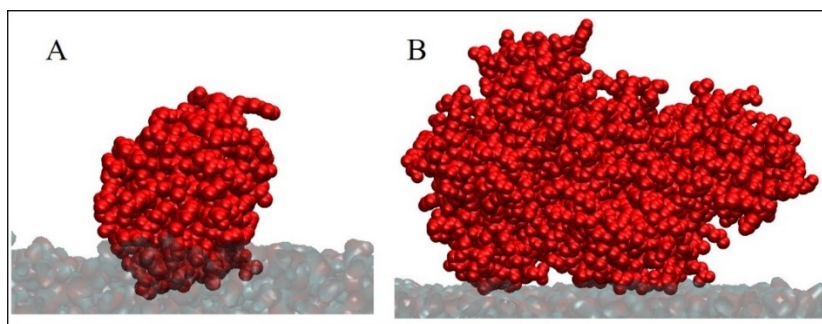


Fig. S11 Snapshots of A): a LYZ molecule or B): a HSA molecule on PMMA. Proteins are in red, while PMMA in grey.

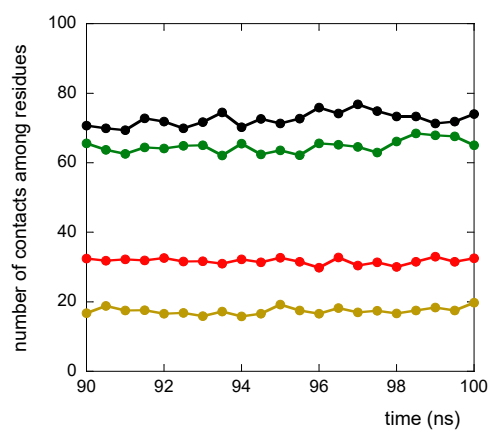


Fig. S12 Average numbers of residues belonging to different proteins at distances less than 0.5 nm in the last 10 ns of simulation time; (red): HSA on gold; (yellow): HSA on PMMA; (green): LYZ on gold; (black): LYZ on PMMA.

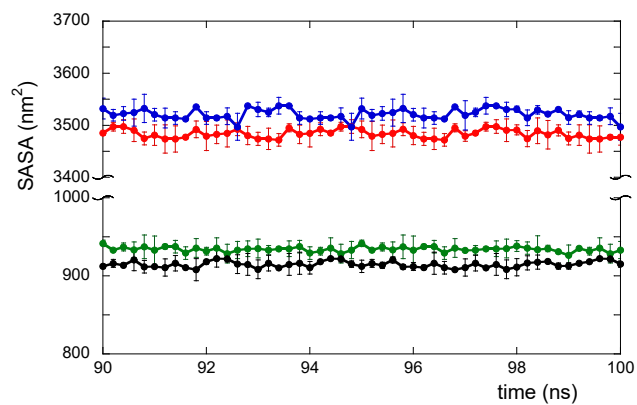


Fig. S13 SASA (Surface Accessible Solvent Area) values for all the proteins in the box in the last 10 ns of simulation; (red): HSA on gold; (blue): HSA on PMMA; (green): LYZ on gold; (black): LYZ on PMMA. Data are the average of the two replicas.

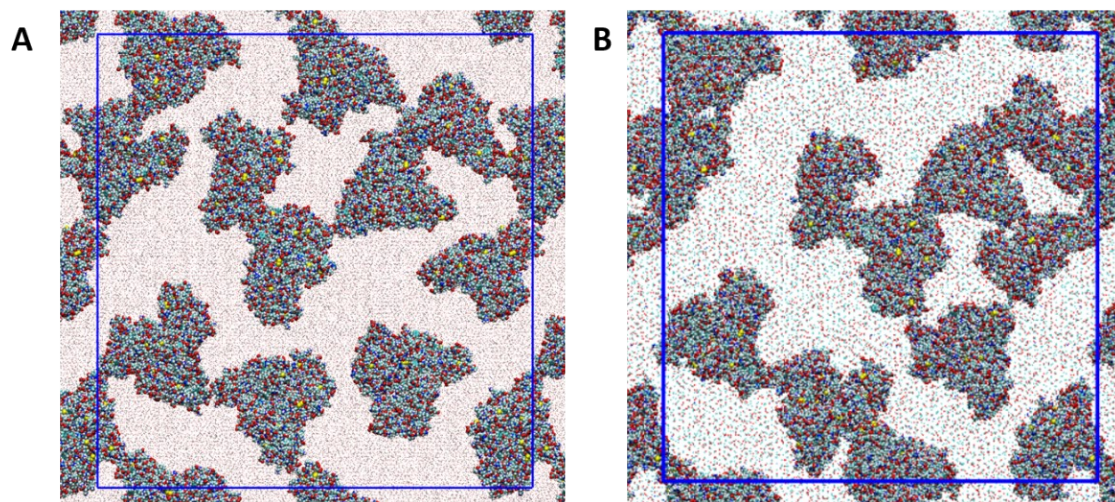


Fig. S14 Top view images of the last snapshot of MD simulations of A) HSA on gold B) HSA on PMMA. Blue square delimits the simulation box.

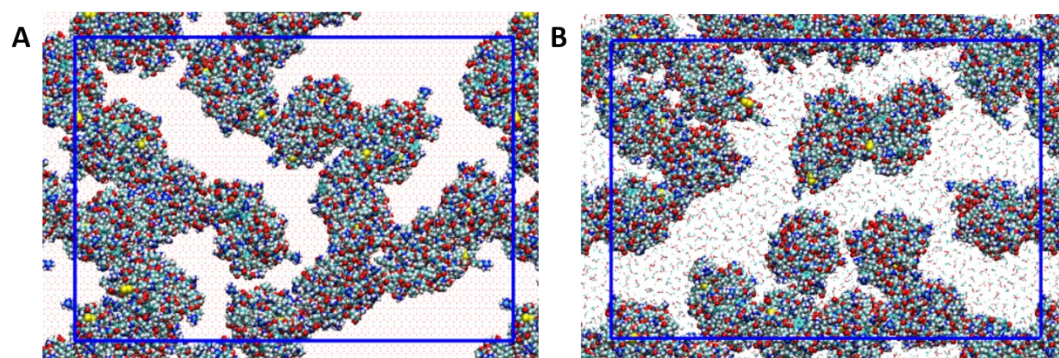


Fig. S15 Top view images of the last snapshot of MD simulations of A) LYZ on Au B) LYZ on PMMA. Blue square delimits the simulation box.

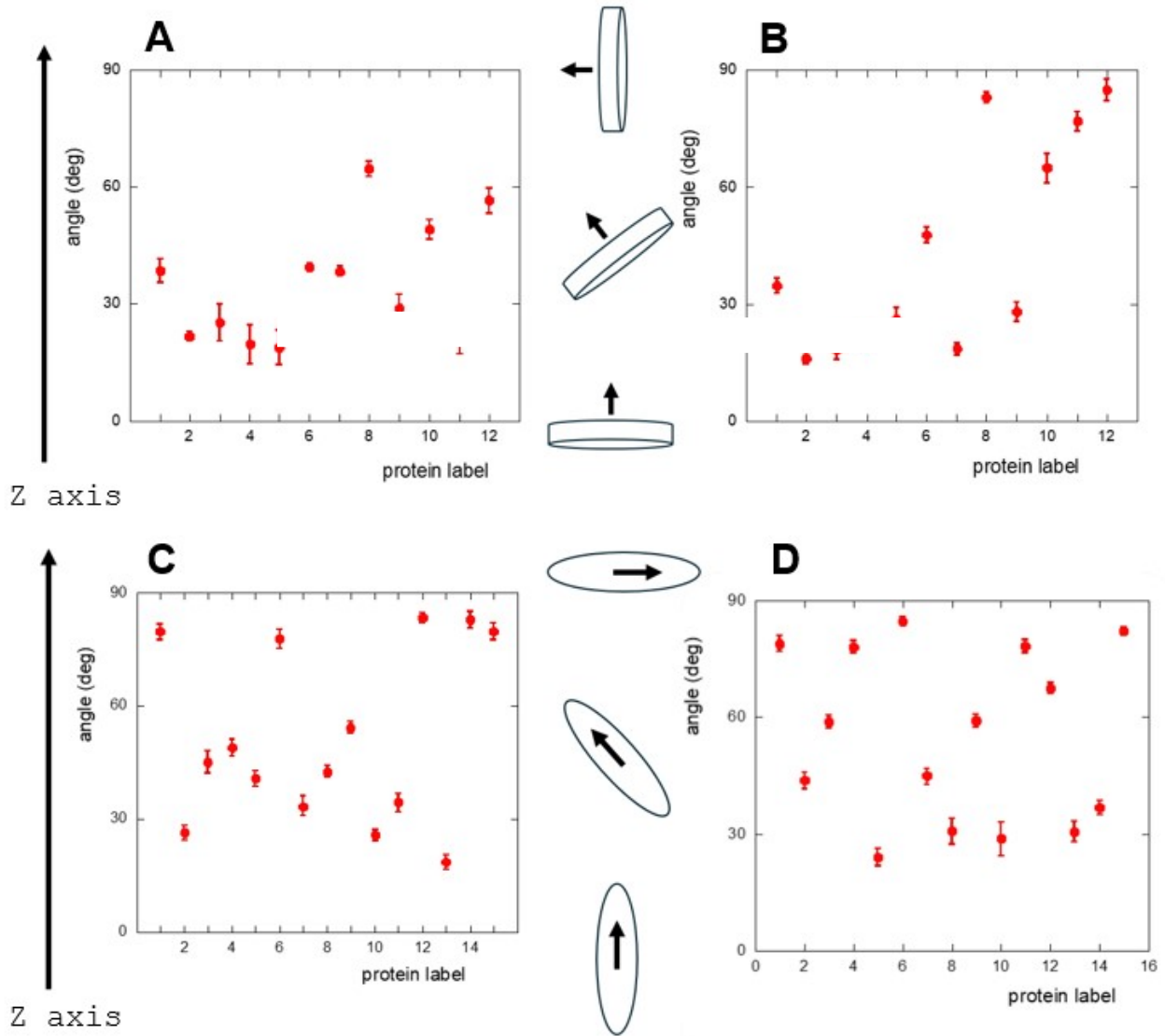


Fig. S16 Angle between the shortest axis of the HSA molecules (top) or the longest axis of LYZ molecules (bottom), and the axis perpendicular to the surface (from left to right and from up to below): HSA on gold, HSA on PMMA, LYZ on gold and LYZ on PMMA.

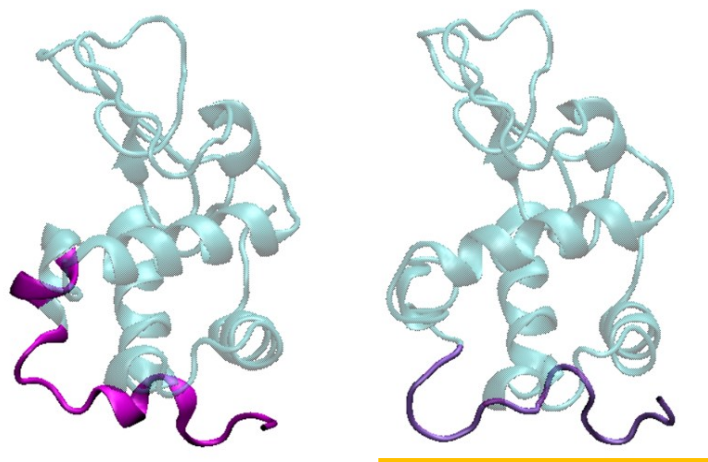


Fig. S17 Conformational changes of the C-terminal of LYZ from solution (*left*) to gold surface (*right*). The yellow line represents the gold surface

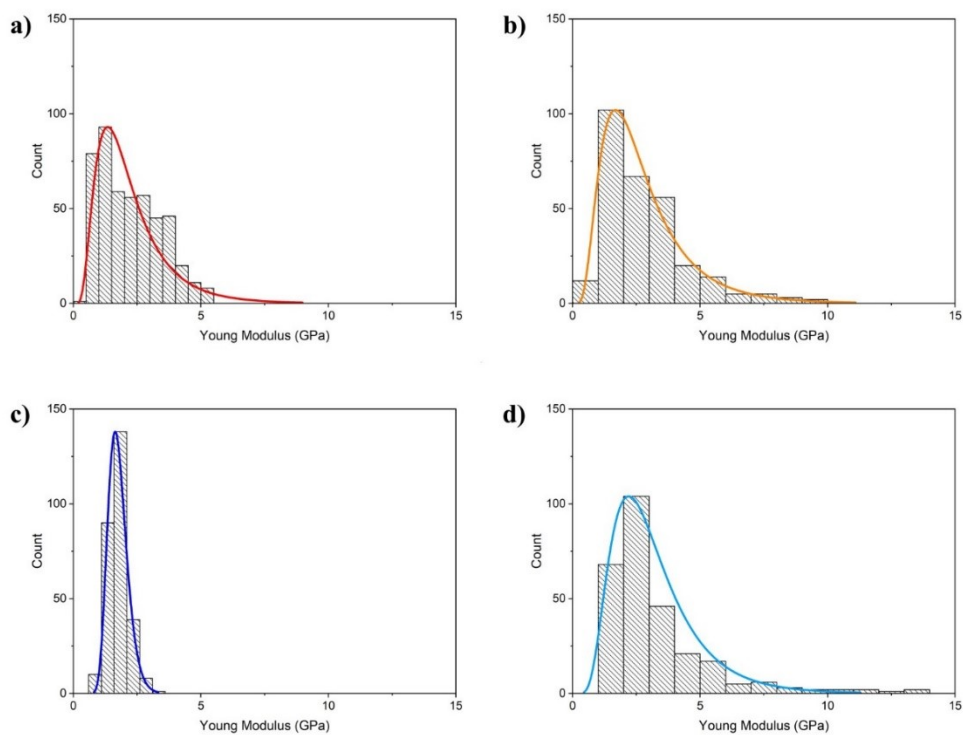


Fig. S18 Young's Modulus distribution for: a) HSA on gold, b) HSA on PMMA c) LYZ on gold and d) LYZ on PMMA, obtained by AFM experiments.

Table S2. Depth dimension of nanowells before (bare) and after protein (HSA and LYZ) adsorption

Nanowells	Depth (nm)
Bare	38.91 ± 2.95
HSA	29.66 ± 4.51
LYZ	41.62 ± 2.10

References

- 1 T. Zhang, T. Wei, Y. Han, H. Ma, M. Samieegohar, P. W. Chen, I. Lian and Y.-H. Lo, *ACS Cent. Sci.*, 2016, **2**, 834–842. (*it is the ref. n. 30 in the main manuscript*)